The Isobutylene−Isobutane Alkylation Process in Liquid HF Revisited

P. M. Esteves,*,† C. L. Araújo,† B. A. C. Horta,† L. J. Alvarez,‡ C. M. Zicovich-Wilson,§ and A. Ramírez-Solís||

Instituto de Química, Universidade Federal do Rio de Janeiro, Cidade Universitária CT Bloco A, 21949-900, Rio de Janeiro, Brazil, Instituto de Matemáticas, Unidad Cuernavaca, Universidad Nacional Autónoma de México, Av. Universidad s/n, 62210 Cuernavaca, Morelos, México, Depto. de Física, Facultad de Ciencias, Universidad Autónoma del Estado de Morelos. Av. Universidad 1001, Cuernavaca, Morelos. 62210. México, and Laboratoire de Physique Quantique, IRSAMC. Université Paul Sabatier, 31062 Toulouse, France

Received: March 28, 2005; In Final Form: May 2, 2005

Details on the mechanism of HF catalyzed isobutylene−isobutane alkylation were investigated. On the basis of available experimental data and high-level quantum chemical calculations, a detailed reaction mechanism is proposed taking into account solvation effects of the medium. On the basis of our computational results, we explain why the density of the liquid media and stirring rates are the most important parameters to achieve maximum yield of alkylate, in agreement with experimental findings. The ab initio Car−Parrinello molecular dynamics calculations show that isobutylene is irreversibly protonated in the liquid HF medium at higher densities, leading to the ion pair formation, which is shown to be a minimum on the potential energy surface after optimization using periodic boundary conditions. The HF medium solvates preferentially the fluoride anion, which is found as solvated $[FHF]^-$ or solvated $F^-\cdot(HF)_3$. On the other hand, the *tert*-butyl cation is weakly solvated, where the closest HF molecules appear at a distance of about 2.9 Å with the fluorine termination of an HF chain.

I. Introduction

The isobutylene−isobutane alkylation process is a very important industrial process,[1] being responsible for the production of high octane number gasoline, which has as the main component isooctane. Liquid HF or H_2SO_4 can be used as catalysts for this reaction. Nevertheless, because of the highly corrosive nature of these media, associated environmental problems, and intrinsic danger in handling these materials,[2] especially in the case of HF, alternative solutions to replace these catalysts for this process are being actively searched for in the petroleum industry.[3] However, many problems arise in finding good heterogeneous catalysts for this reaction.[4] Usually, they are rapidly deactivated yielding oligomeric olefins instead of the desired branched alkane as the product.[1] It arises that a better understanding of the catalytic activity in liquid acid media is necessary to design more suitable alternative catalysts for this reaction. Recently, Olah and co-workers have shown that amine-$(HF)_n$ ionic liquids (onium polyhydrogen fluorides) and their polymeric analogues are interesting alternatives to liquid HF, affording alkylates of good quality, with research octane number (RON) ranging from 91 to 94.[3b]

Because of the complexity of the problem, few studies, especially from the theoretical point of view, have been performed in this system. From the theoretical point of view, no studies taking into account realistic inclusion of the solvation effects of the carbocations formed into the liquid HF medium, fundamental to properly describe these reactions, have so far been performed.

It is generally accepted[5] that this reaction basically involves three main steps: the initial formation of a carbenium ion (initiation), the attack of this cation by an olefin (alkylation), and a termination step (hydride transfer) that affords the respective alkane, usually isooctane in the case of use of isobutylene, regenerating the initial carbenium ion in a self-catalytic way. The optimum acidity range for this reaction is $-13 < H_o < -11$.[6] Moreover, the liquid acid medium also provides a suitable polar reaction environment, wherein the carbenium ions can be easily formed and stabilized. Another interesting aspect is that the isobutylene−isobutane alkylation reaction does not yield alkylates (the desired products) if reactants are used in the gas phase, either in liquid or using most of the possible heterogeneous catalysts. Therefore, a particularly interesting result is that HF is not a good catalyst if it is used in the gas phase. These facts clearly indicate that the bulk acidity and the solvent effects play crucial roles in this process.

To provide a better understanding on how solvent effects influence this important reaction, we performed a theoretical study, using first-principles simulation techniques for the isobutylene−isobutane alkylation process in liquid HF. For this, we performed Car−Parrinello molecular dynamics as well as conventional periodic and molecular density functional theory (DFT) studies concerning the isobutylene−isobutane alkylation process.

II. Method and Computational Details

To study the mechanism of alkylation, we direct our attention to the reactions shown in Scheme 1 within liquid HF. We

* To whom correspondence should be addressed. E-mail: pesteves@iq.ufrj.br.
† Universidade Federal do Rio de Janeiro.
‡ Universidad Nacional Autónoma de México.
§ Universidad Autónoma del Estado de Morelos.
|| Université Paul Sabatier. On sabbatical leave from Depto. de Física, Facultad de Ciencias, Universidad Autónoma del Estado de Morelos.

10.1021/jp051567a CCC: $30.25
Published on Web 06/09/2005

SCHEME 1: General Mechanistic Picture for the Isobutylene/Isobutane Alkylation Reaction[a]

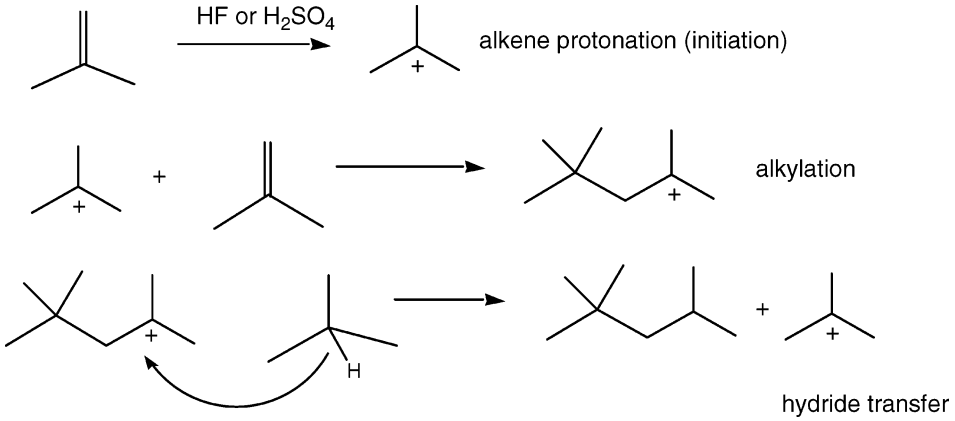

[a] Note the absence of the solvation effects in this widely accepted but very crude picture.

investigated the dynamical behavior of the interaction of molecules of isobutylene in liquid HF using different approaches. First, Car−Parrinello molecular dynamics (CPMD) simulations[7] in a periodic cubic unit cell containing different numbers of isobutylene and HF molecules were done, using the CPMD code.[8] Second, from the trajectories thus generated, we selected the lowest energy configuration and performed periodic quantum chemical geometry optimizations using both plane waves with the BLYP functional and atomic orbital (AO) basis sets, using the CRYSTAL code[9] and the B3LYP functional.[10] The last approach was also used to perform conventional B3LYP-DFT calculations[10] on cluster models mimicking microsolvation using the Gaussian98 package.[11] The use of two different exchange-correlation functionals was deemed necessary to compare and to assess the reliability of the results.

We started by performing the CPMD simulations of liquid HF considering a 10 Å cubic unit cell containing 25 HF molecules, subject to periodic boundary conditions, following the procedure previously reported and with the same time step.[12] Temperature was controlled using the Nosé−Hoover scheme[13] and was kept constant at 300 K. This box size affords approximately the density of anhydrous HF at 19.5 °C (d_{exp} = 0.957 g/mL). After thermal equilibrium for pure HF was achieved, one of the HF molecules was replaced by one isobutylene molecule. The resulting density value (0.895 g/mL) is intermediate between the densities of liquid HF (d_{exp} = 0.957 g/mL) and isobutylene (d_{exp} = 0.588 g/mL). A thermal Boltzmann distribution at 300 K was used to generate the initial velocities. A set of plane waves (PW) with an energy cutoff of 90 Ry was used as the basis set for the Kohn−Sham calculations (using the BLYP functional), jointly with Troullier−Martins pseudopotentials[14] using the Kleinman−Bylander separation scheme[15] for the representation of the core electrons of all the C and F atoms. For the hydrogen atoms, a von Barth−Car norm-conserving pseudopotential was used.[16]

Previous CPMD works have recently been published concerning the structure and dynamics of liquid HF[14,17] as well as fully ab initio MP2 optimized geometries for HF clusters,[18] showing good agreement with experimental data.[19] For this reason, we decided to test several combinations of the available pseudopotentials and PW cutoff energies to reproduce at best the MP2 geometries, at the CPMD level, of clusters containing one, two, and seven HF molecules (this last one in a cyclic configuration). Our results were also compared with the known experimental geometries.[19−21] This comparison allowed us to assess that the chosen combination of pseudopotentials and a 90 Ry cutoff were the ones that best reproduced the reference structures.

In each trajectory step, properties obtained from the wave function, such as energies, total dipole moment, and the atomic velocities, were used for the calculation of other properties. The fictitious mass of the electrons, a parameter that is necessary to define Car−Parrinello type molecular dynamics, was chosen as 800 au. Other authors have used this value successfully before.[14,19]

After isobutylene insertion into preequilibrated liquid HF, a total time of 25 ps of simulation was performed. The CPMD simulations of these systems, one which contains 62 atoms (i-C_4H_8 + 25HF) and the other with 74 atoms (2 i-C_4H_8 + 25HF), each took more than 34 days of parallel CPU time running on 12 Power4 processors of the IBM-p690 32-processor supercomputer at UAEM, using 4GB of RAM; each time step took about 12 wall seconds, with a Kohn−Sham energy and gradient calculation. The time step (Δt) for the integration of the equations of motion used was 0.12 fs to guarantee the propagation of the coefficients of the electronic KS orbitals in a stable manner, thus keeping the trajectory close to the ground-state Born−Oppenheimer surface. After obtaining the CPMD trajectory, the lowest energy structure was located, and geometry optimization was done from this point using the same PW basis and periodic boundary conditions through the conjugated gradient scheme.[22] This was done to obtain the geometries of the solvated species that will help us to determine the role of the solvent effects on those species, which are certainly crucial in this reaction. Complementary ab initio periodic and molecular calculations with AO basis sets were done for the same low-energy structures to have equivalent results from another theoretical framework, which allows us to better assess the accuracy of the PW delocalized description.

Both for the periodic as well as for the molecular DFT cases, the geometries of all investigated species were obtained without any geometrical restrictions imposed and were characterized as true intermediates or transition states in the potential energy surface, respectively, by the absence or presence of imaginary frequencies in the corresponding vibrational analysis. The cluster DFT calculations of reactants and products in the gas phase without periodic boundary conditions were performed at the B3LYP/6-311++G**//B3LYP/6-31++G** level. Zero-point energy (ZPE) and finite temperature corrections at 298 K and 1 atm were computed employing the harmonic oscillator and the ideal gas approximations and using the vibrational

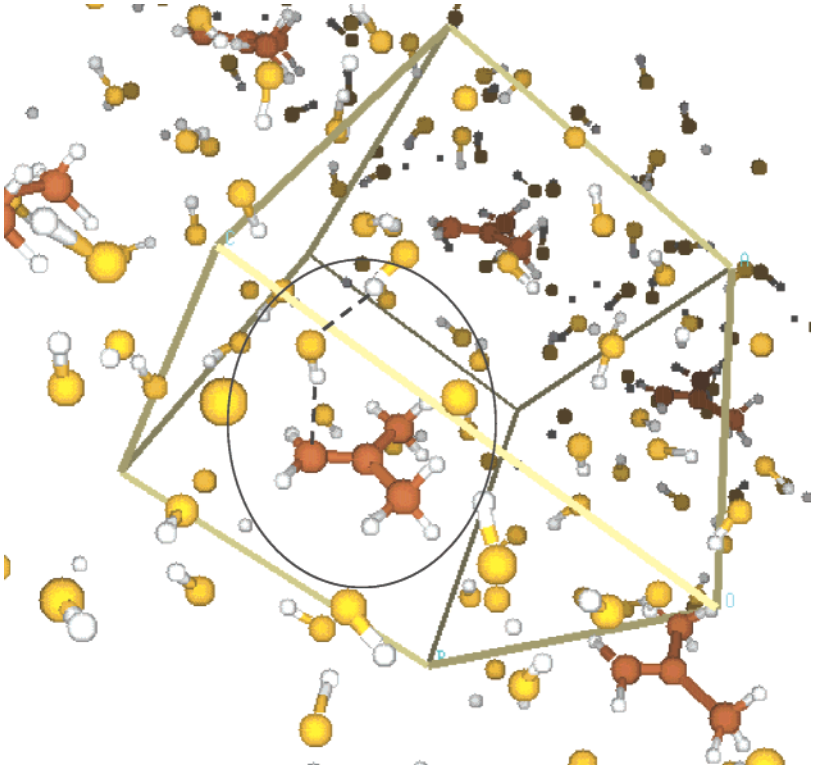

Figure 1. Optimized CPMD periodic BLYP structure of the lowest energy structure found in the CPMD trajectory for *i*-C_4H_8 + 24HF. Note the π-complex thus formed.

frequencies calculated at the B3LYP/6-31++G** level. Relative energies were calculated from these values and correspond to 298 K and 1 atm.

Periodic B3LYP calculations were performed with a standard 6-31G** basis set. Although this basis set level is lower than that used for the clusters, it is suitable for the present study for two reasons: (1) It is well-known that the basis set saturation is attained faster in periodic systems than in molecules because of the superposition of the tails of the infinite set of AOs; therefore, it is expected that the quality of the present basis set will be enhanced in periodic calculations. (2) This basis set permits to perform full geometry optimizations and vibrational analysis, despite the number of atoms per unit cell (substantially larger than in the clusters), and the absence of point symmetry makes these calculations very costly in computational resources. Concerning the numerical parameters of the CRYSTAL calculations, eight points and the standard tolerances were used for sampling in the Brillouin Zone and for the integral evaluations, respectively. Geometry optimizations were carried out using analytical gradient methods as implemented in CRYSTAL03,[23] while vibrational frequencies were computed with a recent implementation[24] in a developing version of the program.

III. Results and Discussion

(a) *i*-C_4H_8 + 24 HF. In this CPMD simulation, we observed the formation of a π-complex where one of the HF molecules is more closely coordinated, in average, to the CH_2 moiety of the double bond.

The HF molecule directly involved in the complex is the last one of a one-dimensional hydrogen-bonded HF chain. Figure 1 shows the optimized CPMD periodic BLYP structure of the lowest energy structure for this trajectory. This complex remains stable during most of the simulation. An interesting feature found was that the density of this system (0.895 g/mL), which is somewhat lower than liquid HF (0.957 g/mL), does not lead to carbenium ion formation during the simulation time. This can explain why the reaction does not lead to alkylates when the reactants (isobutylene, isobutane, and HF) are all in the gas phase. In this case, the only products found are unsaturated oligomers. Thus, the increase of the pressure in the system, leading to an increase of density, forces the system to be in the liquid phase, which may favor the protonation of the isobutylene and should improve the reaction yields. To simulate that, we decided to increase the density of the system by the addition of another HF molecule, which gives a system containing 25 HF and 1 isobutylene molecules. The resulting density is 0.929 g/mL, closer to that of liquid HF (0.957 g/mL). This will be discussed in the next section.

For comparison purposes, we also performed calculations of the species resulting from the interaction of an isobutylene molecule with a variable number ($n = 1-6$) of HF molecules with conventional ab initio techniques at the B3LYP/6-311++G**//B3LYP/6-31++G** level. Figure 2 shows the results for solvation of isobutylene with five HF molecules. The other cases can be found in the Supporting Information section. Our calculations indicate that even with the presence of a few HF molecules, there is only formation of a π-complex in which the olefin is not protonated. There is no carbenium ion formation on the potential energy surface despite the fact that we were able to obtain a transition state for protonation. We found that the protonation enthalpy, from the π-complex in these cluster calculations, is 9.8 kcal/mol at B3LYP/6-311++G**//B3LYP/6-31++G** level considering an unbranched HF chain (Figure 2, top). However, this value drops to 1.7 kcal/mol when the HF chain is branched (Figure 2, bottom). A value of 28.6 kcal/mol for protonation of ethylene by an HF dimer at B3LYP/6-31G** has been reported,[25] somewhat higher than the values found here. This reflects the stability of the carbenium ion on the transition-state energy and the effect of lower solvation on the ethylene case. These results indicate that solvation effects

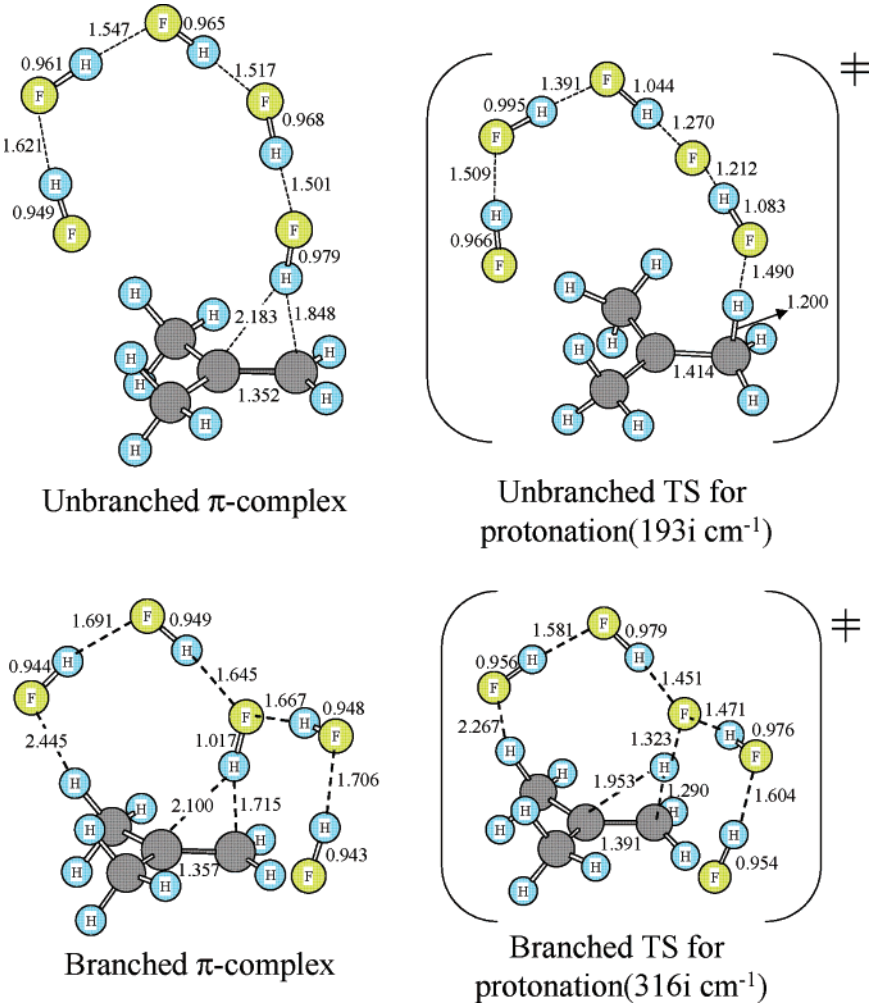

Figure 2. Selected geometries for the complex isobutylene·(HF)$_n$, ($n = 5$) calculated at the B3LYP/6-31++G** level, and the respective transition states for double bond protonation with (a) an unbranched HF chain (top) and (b) a branched HF chain (bottom).

TABLE 1: Thermodynamic Quantities for the Protonation of Isobutylene with Unbranched and Branched HF Chains

	$\Delta H^{\ddagger}$ (298 K) (kcal/mol) $\epsilon = 1$	$\Delta H^{\ddagger}$ (298 K) (kcal/mol) $\epsilon = 78.39$ (PCM)	$\Delta S^{\ddagger}$ (298 K) (cal/mol·K) $\epsilon = 1$	$\Delta G^{\ddagger}$ (298 K) (kcal/mol) $\epsilon = 1$	$\Delta G^{\ddagger}$ (298 K) (kcal/mol) $\epsilon = 78.39$ (PCM)
unbranched	9.8	0.6	−10.12	12.9	3.6
branched	1.7	−2.4	−9.54	4.5	0.5

are crucial for the formation of this ion, as it could be intuitively anticipated. However, entropic factors are also important in this process. For the reactions shown in Figure 2, the ΔS(298 K) are −10.1 cal/mol·K and −9.5 cal/mol·K, respectively, for the case of the protonation with the unbranched and the branched chains. The consideration of entropy allows the calculation of ΔG(298 K), which in this case is 12.9 and 4.5 kcal/mol, for the unbranched and branched chains, respectively. A way of considering these effects in the calculation is using the polarizable continuum models (PCM),[26] considering water as the solvent, since its dielectric constant ($\epsilon_{H2O} = 78.39$) is quite close to the one of liquid HF ($\epsilon_{HF} = 83$), thus mimicking the effect of the highly polar medium, which contains basically liquid HF. We carried out a single-energy calculation on the geometry previously obtained in a vacuum (PCM/B3LYP/6-311++G**//B3LYP/6-31++G**) and observed that the enthalpy for protonation of isobutylene decreases with the inclusion of these effects. Table 1 summarizes these results.

In summary, our calculations indicate that whenever the system has few HF molecules, there is formation of a π-complex, and the olefin is not protonated. However, the increase of the number of HF molecules in the system promotes the formation of a carbenium ion as long-lived species in this medium, this also being a minimum on the potential energy surface. This shows that solvation effects are crucial for the formation of this ion, as could be expected. The driving force for the protonation of the olefin affording the carbocation, indicated by both CPMD and conventional DFT calculations, is the strong solvation of the fluoride, since the carbocation is only slightly solvated. Thus, this result provides an explanation as to why the alkylation reactions do not take place into the gas phase, where only oligomers are formed, as it will be discussed later in the text.

The hydride transfer process was also calculated at the same level of theory. This was done by studying the attack of an isobutane molecule on a carbenium ion. In this case, we found that in the gas phase a carbonium ion is formed, which contains an uncommon linear three-center two-electron bond, which perhaps may not exist as an intermediate in true solvation conditions. However, the analysis of the energetics of its formation can give us an idea of how difficult the hydride transfer step is. The hydride transfer from isobutane to the *tert*-

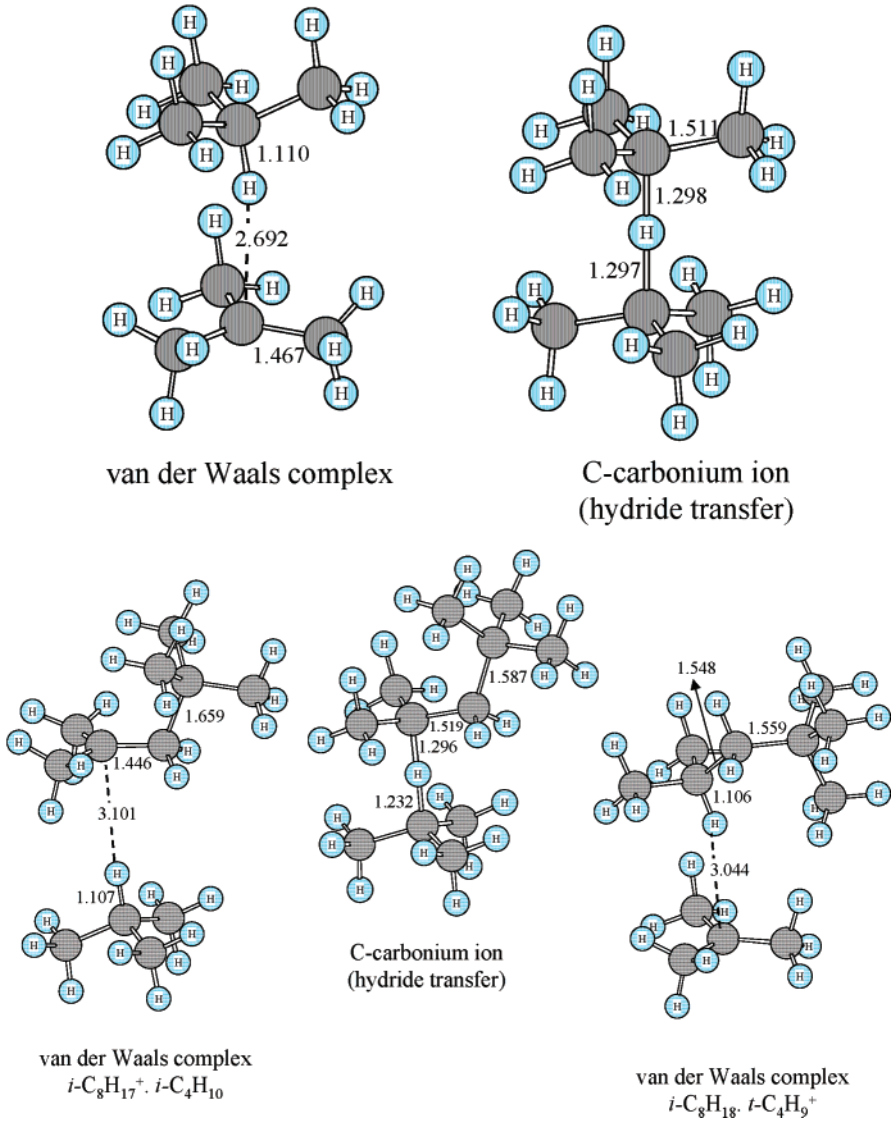

Figure 3. The hydride transfer process between an isobutane molecule and a *tert*-butyl cation (top left) through a C-carbonium ion intermediate (top right) and an isobutane and isooctyl cation (bottom left), through the respective $C_{12}H_{27}^+$ carbonium ion (bottom center), leading to isooctane and another *tert*-butyl cation (bottom right).

butyl cation in gas phase, leading to the formation of the C-carbonium ion, is exothermic by 3.7 kcal/mol at B3LYP/6-311++G**//B3LYP/6-31++G** level. The C-carbonium ion was shown to be a minimum on the potential energy surface by vibrational analysis. Details about the geometry, especially concerning the C-carbonium ion, can be found in Figure 3. This shows that the process is favorable in the gas phase and should not involve energy barriers, in enthalpic terms. However, if entropy is taken into account, the formation of the carbonium ion should be an unfavored process, since the number of particles decreases when going from reactants to products. Actually, our cluster DFT calculations indicate that this process has a $\Delta H^{298K} = -3.7$ kcal/mol and a $\Delta S^{298K} = -20.75$ cal/mol K, resulting in a $\Delta G^{298K} = 2.5$ kcal/mol in the gas phase ($\epsilon = 1$), indicating a small energy barrier for the reaction to take place. In the liquid phase however, solvent effects can significantly modify these quantities. A single-point energy calculation using the polarizable continuum models (PCM), considering water ($\epsilon = 78.39$) as the solvent to mimic the highly polar HF medium ($\epsilon = 83$), at the B3LYP/6-311++G**//B3LYP/6-31++G** level, showed that the carbonium ion formation from its van der Waals precursor is endothermic by 0.5 kcal/mol. Considering the solvent effects (PCM) and entropy factors, the energy barrier for the hydride transfer increases to 6.7 kcal/mol (ΔG^{298}). Thus, this barrier is higher than for the olefin protonation ($\Delta G^{298} = 0.5$ kcal/mol), computed using the same hypothesis. In the case of the hydride transfer from the isobutane to the isooctyl cation, these differences increase even more, since the latter is more stable than the *tert*-butyl cation. It was also possible to find a carbonium ion as a minimum on the potential energy surface for the hydride transfer from an isobutane molecule to the isooctyl cation. Its optimized geometry, as well as the corresponding van der Waals complexes, is shown in Figure 3. The energy barrier for this reaction actually increases in relation to the one involving the t-$C_4H_9^+$ and i-C_4H_{10}. For the gas-phase reaction ($\epsilon = 1$), the $\Delta G^{298} = 9.7$ kcal/mol, which goes to 12.8 kcal/mol when solvent effects are included (PCM). This confirms the hypothesis that the rate-determining step in this process is the hydride transfer. The data are summarized in Table 2.

(b) i-C_4H_8 + 25HF. Upon the addition of the 25th HF molecule in the system mentioned above, the CPMD simulation showed that isobutylene is irreversibly protonated after only 5 ps, forming a *tert*-butyl cation which is stable and persistent throughout the simulation time (25 ps). This is an indication that this species can have a relatively long lifetime in this

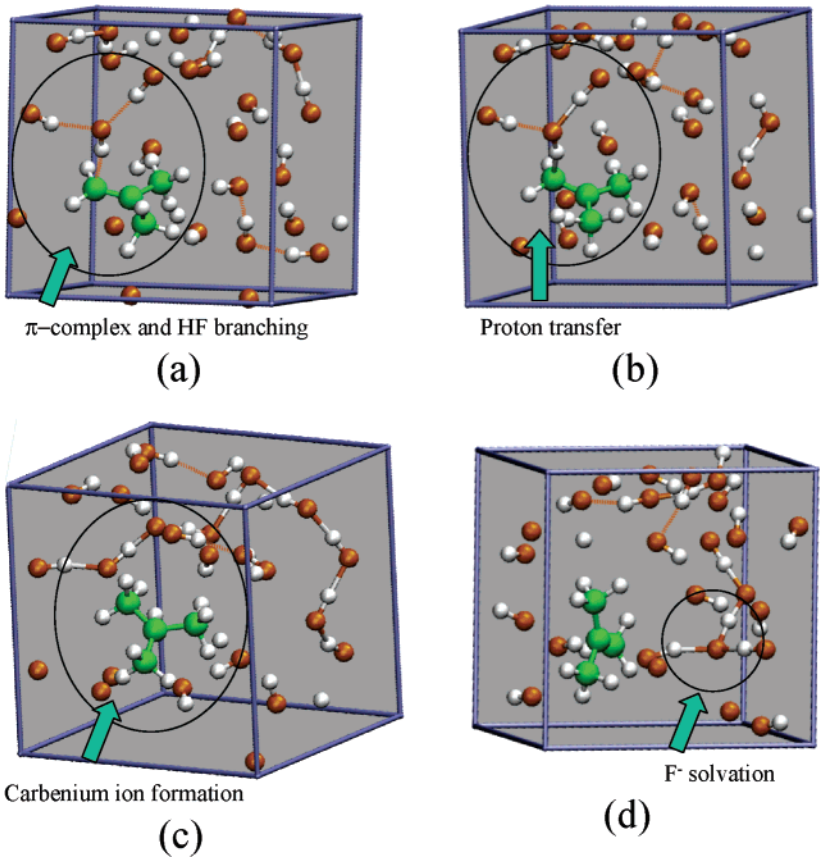

Figure 4. Four snapshots of the dynamics of protonation of one isobutylene molecule in a box containing 25 HF molecules: (a) before the approach of the second HF molecule leading to a branched HF chain; (b) during the proton transfer; (c) the resulting solvated carbocation; and (d) solvation of the fluoride.

TABLE 2: Thermodynamic Data for the Reaction of Hydride Transfer

	ΔH (298 K) (kcal/mol) $\epsilon = 1$	ΔH (298 K) (kcal/mol) $\epsilon = 78.39$ (PCM)	ΔS (298 K) (cal/mol·K) $\epsilon = 1$	ΔG (298 K) (kcal/mol) $\epsilon = 1$	ΔG (298 K) (kcal/mol) $\epsilon = 78.39$ (PCM)
$t\text{Bu}^+ \cdot i\text{C}_4\text{H}_{10} \rightarrow [t\text{Bu}...\text{H}...t\text{Bu}]^+$	−3.7	0.5	−20.75	2.5	6.7
$t\text{Bu}^+ \cdot i\text{C}_8\text{H}_{18} \rightarrow [t\text{Bu}...\text{H}...t\text{-C}_8\text{H}_{17}]^+$	5.3	8.5	−14.67	9.7	12.8

medium, which now has a density of 0.929 g/mL. The driving force for the protonation is the attachment of a second hydrogen-bonded HF to the fluorine atom of the terminal HF molecule that is directly involved in the π-complex, describing a branching in the HF chains. This branch stabilizes the fluoride anion being formed during the protonation, which allows the process to take place quickly at 300 K. Figure 4 shows four snapshots, one before the approach of the second HF molecule, one during the proton transfer, and one after this has taken place. This whole process lasts for 0.48 ps and occurs before thermalization of the system, which is achieved at around 7.5 ps. The conventional cluster DFT calculations show that the energy barrier for the protonation is about 9.8 kcal/mol, for single-chained HF, and 1.7 kcal/mol for the branched chain (see Figure 2), in complete agreement with the molecular dynamics picture.

The lowest energy structure found in the trajectory was located and used to perform periodic PW-BLYP (CPMD) and AO B3LYP (CRYSTAL) geometry optimizations. The periodic optimized structure is shown in Figure 5; however, the PW optimized structure is not qualitatively very different from this one. Even after the geometry optimization procedure, in the resulting structure the *tert*-butyl carbenium ion is present, indicating again that this is a long-lived species in this medium. The corresponding vibrational analysis from the periodic AO optimization shows that the solvated *tert*-butyl cation is a true minimum on the potential energy surface. Bond lengths and angles are compatible with the values found from the gas-phase cluster ab initio calculations,[27] as well as with structures obtained from experimental single-crystal X-ray diffraction studies.[28]

The main idea drawn from all these calculations is that the strong solvation of the fluoride anion is the driving force for the carbocation formation, since no specific interaction with solvent (HF) molecules or even strong solvation of the carbocation exists in this medium. The HF medium solvates preferentially the fluoride anion, which is found as solvated $[\text{FHF}]^-$ or solvated $\text{F}^- \cdot (\text{HF})_3$.

On the other hand, the *tert*-butyl cation is weakly solvated, since the closest HF molecule appears at a distance of about 2.8 Å with the fluorine termination of an HF chain. The remaining F−C distances are larger than 3.0 Å. This is the reason the alkylation reaction does not take place in the gas phase, where only oligomer formation is found instead of the formation of the dimer of the alkane (isooctane). The liquid HF phase is a sine qua non condition for the carbenium ion formation.

To have another insight into the structure of the solution, the pair radial distribution functions were calculated from the molecular dynamics trajectories. Figure 6 shows the relevant pairs, namely, F−F, H−H, C−F, and F−H. Comparison to their

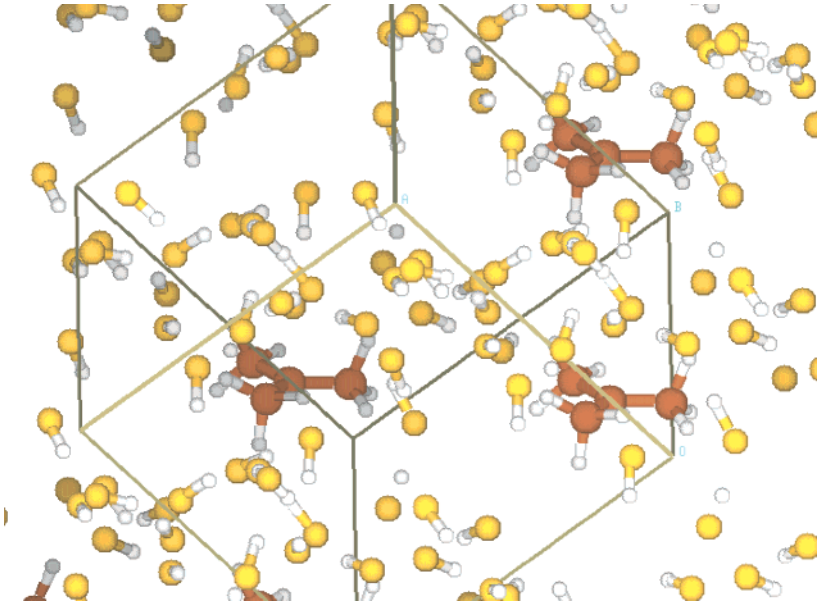

Figure 5. Optimized CPMD BLYP structure of the lowest energy structure found in the *i*-C_4H_8 + 25HF CPMD trajectory. The *tert*-butyl cation remains in this medium as a persistent long-lived species.

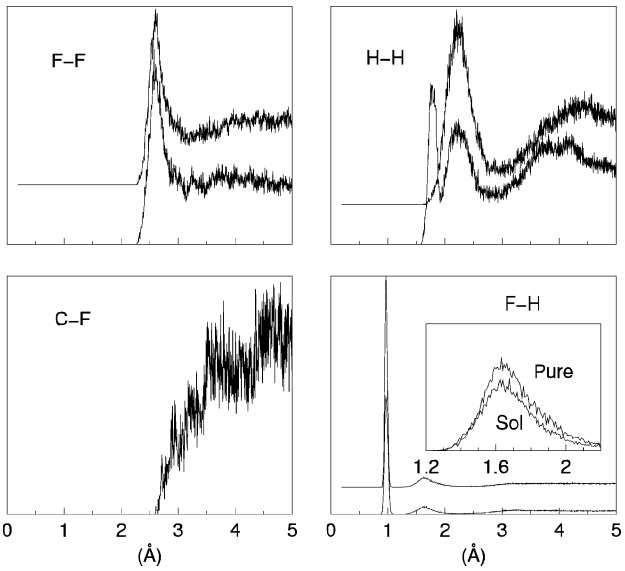

Figure 6. Radial distribution functions of *tert*-butyl solution compared with the corresponding pairs of pure HF liquid. Pure liquid functions are shifted upward. Inset of the F−H function shows the second peak with no shifting.

corresponding functions for the pure HF liquid at the same thermodynamic conditions is shown (except obviously for C−F).

The radial distribution functions (g(r)) for the pairs F−F and H−H for the two cases are essentially the same except for the appearance of an H−H peak characteristic of the intramolecular distance of the *tert*-butyl cation.

The g(r_{C-F}) has the same structure and meaning as the C−F distances in the optimized geometry. This is another indication that the solvent cage is larger than expected in a strong solvation situation.

The second peak of the g(r_{F-H}) shows a very slight difference because of the presence of the *tert*-butyl cation and the fluoride. The presence of *tert*-butyl and fluoride ions lowers the height of the second peak of the g(r) attributed to the HF hydrogen bond. Therefore, one could expect that in the solution the introduction of the ions diminishes the length of H−F chains.

(c) 2 *i*-C_4H_8 + 22HF. An interesting result comes out from the CPMD simulation where two isobutylene molecules are randomly inserted in the liquid HF medium. To keep the density of the simulation close to the average of the pure compounds, we used 22 HF molecules and 2 isobutylene molecules in the same 10 Å box, which leads to a value of density of 0.922 g/mL. It is observed that both olefin molecules stay most of the time as π-complexes with the HF chains. Nevertheless, after approximately 24 ps of simulation, one of these molecules undergoes protonation, after its closest HF molecule (actually the one that is directly making the π-complex) interacts through a second hydrogen bond with another HF chain. After this second hydrogen bond formation, the protonation takes place promptly, leading to a persistent *tert*-butyl cation in this solution.

(d) 2 *i*-C_4H_8 + 25HF. To check the effect of the increase in the density, we randomly added an *i*-C_4H_8 molecule into the initial configuration used in the *i*-C_4H_8 + 25HF case (see b). This would lead to a greater density (1.022 g/mL), which could be due (in the true reaction medium) to an increase of the pressure of the system. By doing this, a very interesting result comes out from the simulation. In this case, it is observed that both olefin molecules are quickly and irreversibly protonated by the medium (considering the present simulation time), forming two persistent *tert*-butyl cations in this solution. The geometry optimized at the AO periodic B3LYP level starting from the lowest energy structures along the molecular dynamics trajectory is shown in Figure 8. This result corroborates those obtained for the system containing one isobutylene molecule.

This faster protonation process can be attributed to a greater probability of existence of branched HF chains when the HF: isobutylene molar ratio increases from 22:2 to 25:2, which was shown to stabilize the negative charge formed in the liquid HF medium upon isobutylene protonation.

The fluoride anion, which is the carbocation gegenion, is stabilized in this medium as $[F-H-F]^-$ because of its interaction with one HF molecule or is solvated by three HF molecules leading to a $F^-\cdot(HF)_3$ complex. These two species are relatively strongly solvated in the medium, as can be seen in Figure 9. Most of the HF molecules are involved in the solvation of the anion.

All these results indicate that there is no significant concentration of olefins in liquid HF because of the irreversible protonation in this medium in the higher density case. However,

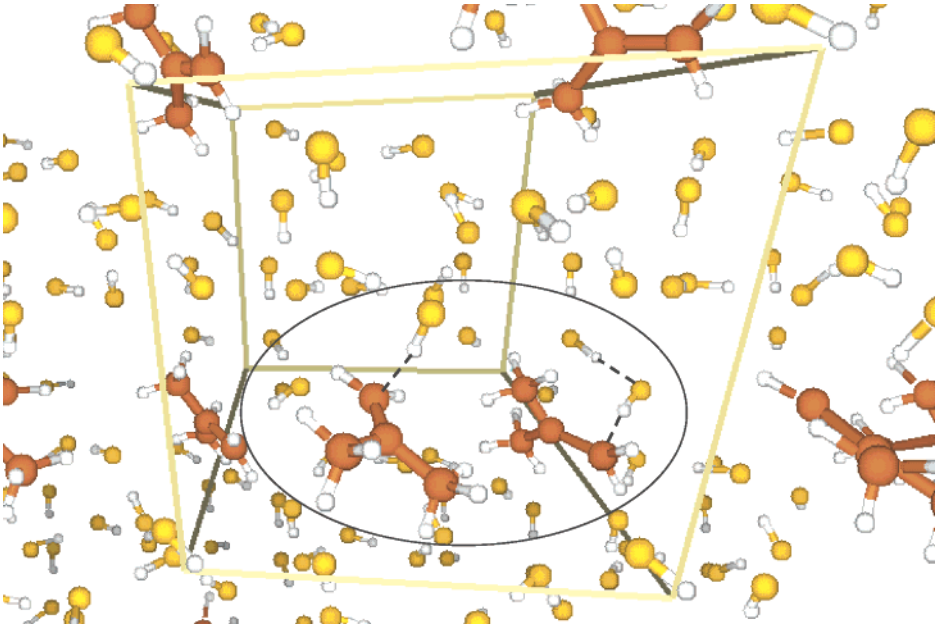

Figure 7. Optimized AO periodic B3LYP structure of the lowest energy structure found in the CPMD trajectory for 2(*i*-C_4H_8) + 22HF, showing the two isobutylene molecules as π-complexes. The protonation of one of the molecules takes place at 24 ps.

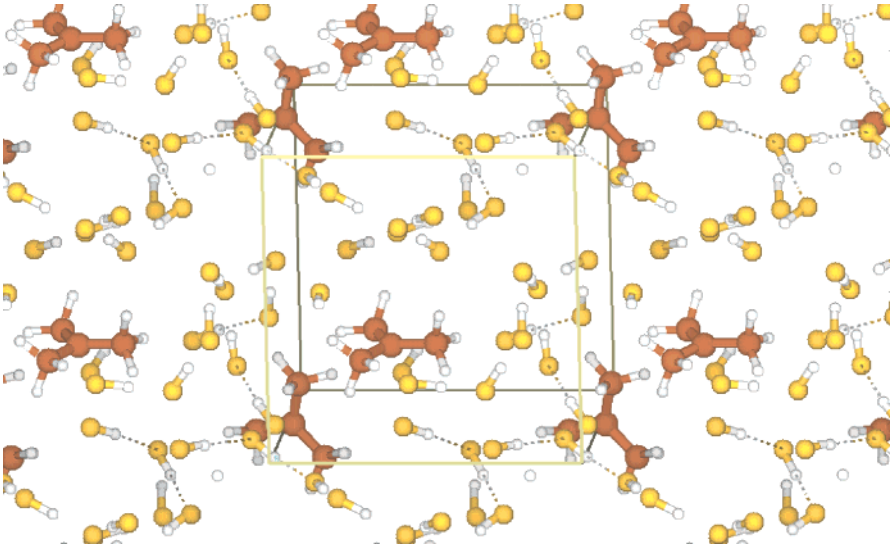

Figure 8. Different perspectives and representations of the geometry obtained after geometry optimization of the lowest energy structure obtained from the CPMD trajectory for 2(*i*-C_4H_8) + 25HF. Two *tert*-butyl cations are formed as stable species in this medium.

when liquid HF and a liquefied solution of isobutylene in isobutane (usually with isobutane:isobutylene molar ratios equal or higher than 10:1) are mixed together, there is separation into two phases, with one of the phases being organic (the solution of isobutylene in isobutane) and the other inorganic (liquid HF). With this experimental information and from the results obtained from our CP molecular dynamics results, we believe that this phase separation is crucial for the success of the medium as the catalyst of choice for the production of alkylated gasoline. The existence of both liquid phases at the usual temperature for this reaction (36 °C) is only possible in sealed vessels, which are subject to pressures higher than the atmospheric, probably leading to higher densities. As indicated by the molecular dynamics calculations, there should not be a significant concentration of isobutylene as an olefin in the HF phase and, at the same time, a significant concentration of the *tert*-butyl cation in the organic phase (isobutane) should not exist either, because of its low ability to solvate charged species (low polarity and low dieleletric constant). Therefore, if the *tert*-butyl cation and isobutylene are in different phases, the natural question arises: where do the reactions that lead to the alkylated products take place? Before trying to answer this question, let us analyze in greater detail the rate expressions for the mechanism shown in Scheme 1. If one assumes that this is a good mechanism scheme for the reaction, the equations of the reaction rates for each of the steps are the following:

$$v_1 = k_1\,[i\text{-}C_4H_8][H^+]\ \text{(protonation step)}$$

$$v_2 = k_2\,[t\text{-}C_4{}^+][i\text{-}C_4H_8]\ \text{(alkylation step)}$$

$$v_3 = k_3\,[i\text{-}C_8{}^+][i\text{-}C_4H_{10}]\ \text{(hydride transfer step)}$$

The rate of the alkylation process is a first-order one with respect to isobutylene and to the carbocation, whereas the hydride transfer step is first-order in relation to the carbocation and to isobutane concentration. Therefore, the carbocation formed in the inorganic phase should be in direct contact with

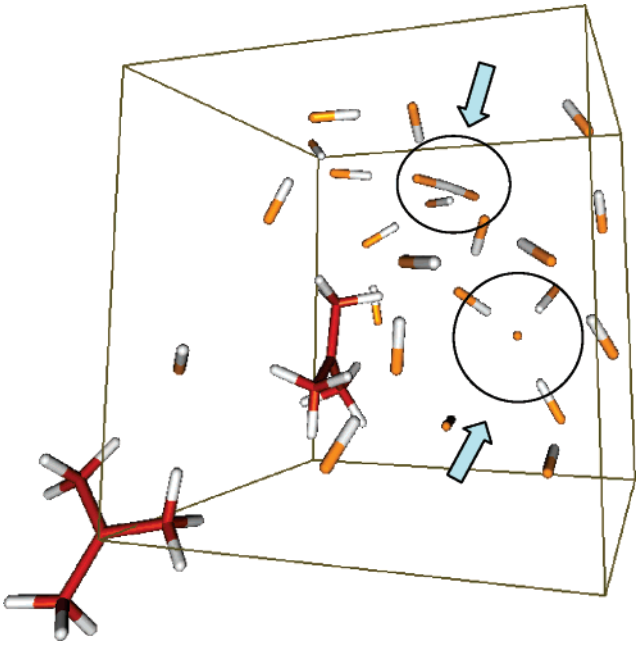

Figure 9. Details on the structure shown in Figure 8 (above). Arrows indicate the position of the two fluoride anions, which compensate for the positive charges of the two carbocations formed. Note the different solvation mechanisms on the two anions.

isobutylene for alkylate formation, which probably occurs in the interfacial region between the two liquid phases. With relation to the intrinsic values of the rate constants, the expected order should be $k_1 > k_2 > k_3$. Thus, on the basis of the kinetic expressions, it should be expected that the undesired oligomerization process should be favored, since the alkylation step is intrinsically faster that the hydride transfer; recall that there must be a hydride transfer to the isooctyl cation to obtain the desired alkane, isooctane. To obtain good yields of isooctane (and other branched alkanes with high octane numbers), it is necessary for the carbenium ion to be alkylated by an olefin molecule and to immediately undergo a hydride transfer reaction with a hydride donor (e.g., isobutane). Otherwise, the resulting carbenium ion will undergo multiple alkylations leading to oligomeric products, which are undesirable. Therefore, the hydride transfer step prevents the isoctyl cation (i-C_8^+) to react with other olefin molecules, preventing the oligomerization process. The oligomeric cation could undergo rearrangements and scissions, yielding smaller carbenium ions and olefins, which are believed to be the source for the alkylated products C5−C7 ("light ends") and C9−C12+ ("heavier ends"). Both light and heavy ends are undesired products, since the former give higher volatility to the final gasoline, leading to problems associated with safety and environmental legislation, especially in the handling of the products in the gas stations. The latter can cause problems in the ignition of the engine, because of the wrong air/fuel composition, as deposit (gum) formation is promoted in the electronic fuel injection system. Thus, all these aspects lead to practical undesired problems.

However, if one considers that this is a process that occurs in a biphasic system, one consisting of liquid HF (inorganic) and the other of the isobutane/isobutylene solution (organic), this promotes a fundamental change in the rates of reaction. In the inorganic phase, there is instantaneous formation of persistent *tert*-butyl cations, but there is no isobutylene present. Isobutylene only exists unprotonated in the organic phase which, in turn, does not contain persistent carbenium ions because of its low dielectric constant. Thus, the alkylation process (rate v_2), although energetically favored in relation to the hydride transfer step, is slowed because of low concentration of one of the species necessary for this step to take place, since those species are separated in different phases. Probably, the only region where the two species coexist, thus favoring alkylation, is at the interface between the two liquid phases. However, in this region the isobutane concentration is high (isobutane:isobutylene molar ratio $\geq$10:1), favoring the hydride transfer step, which depends on the concentration of the carbocation (preferentially the isooctyl cation) and of isobutane (hydride donor) and that leads to the desired products, such as isooctane or other branched alkanes. This local concentration effect of the reactants makes the hydride transfer reaction become a process competitive with the intrinsically fast alkylation step, thus favoring the formation of the alkylated products. This picture is in perfect agreement with the dependency on the yield of alkylated products with the stirring speed of the reaction media. An increase of the yield is observed by increasing the stirring rates, this being a very important operational parameter in the process.[29] The increase of the stirring rate increases the interface area between the two liquid phases and it can promote the interface reaction, thus corroborating our reaction model.

On the basis of the present results, it is possible to understand the reason it is so difficult to design heterogeneous catalysts for this reaction. Since the adsorption step is fundamental in heterogeneous catalysis, by percolating a mixture of isobutylene and isobutane on the catalyst bed, either in the liquefied or on the gas phase or with high isobutane/isobutylene molar ratios, the following problems will be found, which inevitably lead to the oligomer formation:

(a) The adsorption step on the catalyst surface is usually favored by the more polarizable species, which is isobutylene in this case. Thus, there will be a high concentration of the olefin on the catalyst surface, favoring multiple alkylation, which naturally leads to oligomeric products. They will also block the active site, since they will not desorb from it, thus leading to quick deactivation of the catalyst.

(b) The formation of carbenium ions as stable species in the presence of the solid-phase catalyst reaction medium would be difficult in the cases where absence of significant solvation occurs. Thus, this would lead to a decrease on the carbocation concentration and to an increase on that of olefins, favoring even more the alkylation step, leading again to oligomerization and catalyst deactivation.

Analysis of the molecular dynamics results of these species in liquid HF indicates that the stabilization of these species comes from the favorable solvation of the fluoride anion by this medium, because of the formation of $[F-H-F]^-$ and $F^-\cdot(HF)_3$ ions. There does not seem to exist a specific stabilization of the carbocation, which is also not attacked by the medium, which is barely nucleophilic. The formation of a heterogeneous reacting medium containing a two-phase liquid system, therefore, has good qualities for being the best catalyst for this process.

IV. Conclusions

The HF medium is acidic enough to promote and stabilize the *tert*-butyl cation as a long-lived persistent intermediate, because of its high acidity and good solvation ability, especially for the fluoride anion formed in the process. In these conditions, olefin concentration is kept very low, which makes the production of oligomeric species unfavorable, from a reaction rate point of view, compared to the alkylate formation. New hydrogen bonding at the HF end of the π-complex isobutylene:HF, leading

to a branch, leads to the protonation of the olefin, affording a long-lived carbenium ion. The protonation energy is estimated by cluster DFT calcutation to be 9.8 kcal/mol, in the unbranched HF case, and 1.7 kcal/mol, in the case of the branched HF chain.

We propose that alkylation and hydride transfer only take place, yielding the desired products (branched alkanes), on the interface between the organic phase and the liquid HF, since only in this region is there possible contact between the carbocation and the olefin molecules. Considering that the organic phase is basically composed of isobutane (present in at least 10:1 molar ratio in relation to isobutylene), there is a greater probability of the isooctyl cation to react, via hydride transfer, with isobutane, despite possible oligomerization because of the high isobutylene concentration.

Thus, liquid HF plays a very interesting role in this reaction. On one hand, it has enough acidity to displace the isobutylene/t-$C_4H_9^+$ equilibrium to the carbocation side, and it also promotes a phase separation of the carbenium ion and the unprotonated isobutylene, dissolved inside the organic phase containing a high concentration of isobutane and insoluble in the HF phase.

Therefore, we conclude that, to obtain new and efficient catalysts for use in this process under the acid-catalyzed paradigm, it is necessary that this new catalyst favors the hydride transfer reaction rate with respect to the alkylation step.

Since the reaction occurs at the interface between the two liquid phases, we have explained why the process can be improved, affording better quality of products, by increasing the stirring rates in the reaction, which promotes a higher contact surface between the two phases. Our simulations show that increasing the pressure on the reaction to guarantee that the reaction medium has the appropriate density so that it becomes a two-liquid-phase system is also crucial.

In addition, we are proposing here that the existence of oligo- or polymeric carbenium ions and olefins in the HF medium can work as a pool of hydride-donor species, more efficient than isobutane, since those species tend to form larger charge-delocalized structures leading to the production of aromatic molecules (coke precursors). Thus, the existence of these species in the medium should also improve the alkylate quality, in case they do not decrease the acidity of the medium.

Acknowledgment. P.M.E. and B.A.C.H. acknowledge CNPq (PROFIX) and FAPERJ (Brazil) for financial support. A.R.S. thanks support from CONACYT project number 34673-E. C.Z.W. thanks support from PROMEP. We wish to gratefully acknowledge unlimited superscalar processor time on the 32 processor IBM-p690 supercomputer at Universidad Autónoma del Estado de Morelos in Cuernavaca, through "Cómputo Científico" FOMES2000-SEP Project, without which this study could not have been done.

Supporting Information Available. The partial or full molecular dynamics trajectories for all the CPMD simulations and optimized geometries obtained for several isobutylene·$(HF)_n$ complexes, calculated at B3LYP/6-31++G, are available upon request from the authors.

References and Notes

(1) (a) Shreeve, R. N.; Albright, L. F. In *Unit Processes in Organic Chemistry*, 5th ed.; Groggings, P. H., Ed.; McGraw-Hill: Tokyo, Japan, 1958; Chapter 14. (b) Stell, J. *Oil Gas J.* **2001**, *99*, 74.

(2) Segal, E. B. *Chem. Health Saf.* **2000**, *7*, 18.

(3) (a) Corma, A.; Martinez, A. *Catal. Rev. Sci. Eng.* **1993**, *35*, 483. (b) Olah, G. A.; Mathew, T.; Goeppert, A.; Torok, B.; Bucsi, I.; Li, X.-Y.; Wang, Q.; Marinez, E. R.; Batamack, P.; Aniszfeld, R.; Prakash, G. K. S. *J. Am. Chem. Soc.* **2005**, *127*, 5964−5969 and references therein.

(4) (a) Weitkamp, J.; Traa, Y. In *Handbook of Heterogeneous Catalysis*; Ertl, G., Knozinger, H., Weitkamp, J., Eds.; VCH: Weinheim, Germany, 1997; Vol. 4, p 2039. (b) Albright, L. F. *Chemtech* **1998**, 46.

(5) (a) Feller, A.; Zuazo, I.; Guzman, A.; Barth, J. O.; Lercher, J. A. *J. Catal.* **2003**, *216*, 313−323. (b) Feller, A.; Guzman, A.; Zuazo, I.; Lercher, J. A. *J. Catal.* **2004**, *224*, 80−93. (c) Feller, A.; Lercher, J. A. *Adv. Catal.* **2004**, *48*, 229−295.

(6) Olah, G. A.; Batamack, P.; Deffieux, D.; Török, B.; Wang, Q.; Molnar, A.; Prakash, G. K. S. *Appl. Catal. A* **1996**, *146*, 175.

(7) Car, R.; Parrinello, M. *Phys. Rev. Lett.* **1985**, *55*, 2471.

(8) CPMD, Copyright IBM Corp 1990−2004, Copyright MPI für Festkörperforschung Stuttgart 1997−2001, version 3.7.2 (www.cpmd.org).

(9) Saunders, V. R.; Dovesi, R.; Roetti, C.; Orlando, R.; Zicovich-Wilson, C. M.; Harisson, N. M.; Doll, K.; Civalleri, B.; Bush, I.; D'Arco, Ph.; Llunell, M. *CRYSTAL2003, User's Manual*; University of Torino: Torino, Italy, 2003 (http://www.crystal.unito.it).

(10) Becke, A. D. *Phys. Rev. A* **1988**, *38*, 3098. (b) Lee, C.; Yang, W.; Parr, R. G. *Phys. Rev. B* **1988**, *37*, 785. (c) Miehlich, B.; Savin, A.; Stoll, H.; Preuss, H. *Chem. Phys. Lett.* **1989**, *157*, 200.

(11) Frisch, M. J.; Trucks, G. W.; Schlegel, H. B.; Scuseria, G. E.; Robb, M. A.; Cheeseman, J. R.; Zakrzewski, V. G.; Montgomery, J. A., Jr.; Stratmann, R. E.; Burant, J. C.; Dapprich, S.; Millam, J. M.; Daniels, A. D.; Kudin, K. N.; Strain, M. C.; Farkas, O.; Tomasi, J.; Barone, V.; Cossi, M.; Cammi, R.; Mennucci, B.; Pomelli, C.; Adamo, C.; Clifford, S.; Ochterski, J.; Petersson, G. A.; Ayala, P. Y.; Cui, Q.; Morokuma, K.; Malick, D. K.; Rabuck, A. D.; Raghavachari, K.; Foresman, J. B.; Cioslowski, J.; Ortiz, J. V.; Baboul, A. G.; Stefanov, B. B.; Liu, G.; Liashenko, A.; Piskorz, P.; Komaromi, I.; Gomperts, R.; Martin, R. L.; Fox, D. J.; Keith, T.; Al-Laham, M. A.; Peng, C. Y.; Nanayakkara, A.; Gonzalez, C.; Challacombe, M.; Gill, P. M. W.; Johnson, B.; Chen, W.; Wong, M. W.; Andres, J. L.; Gonzalez, C.; Head-Gordon, M.; Replogle, E. S.; Pople, J. A. *Gaussian 98*, Revision A.7; Gaussian, Inc.: Pittsburgh, PA, 1998.

(12) Röthlisberger, U.; Parrinello, M. *J. Chem. Phys.* **1997**, *106*, 4658.

(13) (a) Nosé, S. *J. Chem. Phys.* **1984**, *81*, 511. (b) Nosé, S. *Mol. Phys.* **1984**, *52*, 255. (c) Hoover, W. G. *Phys. Rev. A* **1985**, *31*, 1695.

(14) (a) Troullier, N.; Martins, J. L. *Phys. Rev. B* **1991**, *43*, 1993−2006. (b) Troullier, N.; Martins, J. L. *Phys. Rev. B* **1991**, *43*, 8861−8869.

(15) Kleinman, L.; Bylander, D. M. *Phys. Rev. Lett.* **1982**, *48*, 1425.

(16) Sprik, M.; Hutter, J.; Parrinello, M. *J. Chem. Phys.* **1996**, *105*, 1142.

(17) (a) Kreitmeir, M.; Bertagnolli, H.; Mortensen, J. J.; Parrinello, M. *J. Chem. Phys.* **2003**, *118*, 3639. (b) Raugei, S.; Klein, M. L. *J. Am. Chem. Soc.* **2003**, *125*, 8992.

(18) Rincón, L.; Almeida, R.; García-Aldea, D.; Riega, H. D. *J. Chem. Phys.* **2001**, *114*, 5552−5561.

(19) McLain, S. E.; Benmore, C. J.; Siewenie, J. E.; Urquidi, J.; Turner, J. E. C. *Angew. Chem., Int. Ed.* **2004**, *43*, 1952.

(20) (a) Johnson, M. W.; Sandor, E.; Arzi, E. *Acta Crystallogr., Sect. B* **1975**, *31*, 1998. (b) *NIST Chemistry WebBook, NIST Standard Reference Database Number 69*; Linstrom, P. J., Mallard, W. G., Eds.; National Institute of Standards and Technology: Gaithersburg, MD, March 2003 (http://webbook.nist.gov).

(21) Janzen, J.; Bartell, L. S. *J. Chem. Phys.* **1969**, *50*, 3611.

(22) Fletcher, R. *Practical Methods of Optimization*; Wiley: New York, 1980; Vol. 1.

(23) Doll, K.; Harrison, N. M.; Saunders, V. R. *Int. J. Quantum Chem.* **2001**, *82*, 1.

(24) Pascale, F.; Zicovich-Wilson, C. M.; López-Gejo, F.; Civalleri, B.; Orlando, R.; Dovesi, R. *J. Comput. Chem.* **2004**, *25*, 888−897.

(25) Jursic, B. S. *J. Mol. Struct. (THEOCHEM)* **1998**, *434*, 37.

(26) Cancès, M. T.; Mennucci, B.; Tomasi, J. *J. Chem. Phys.* **1997**, *107*, 3032.

(27) Sieber, S.; Buzek, P.; Schleyer, P. v. R.; Koch, W.; Carneiro, J. W. d. M. *J. Am. Chem. Soc.* **1993**, *115*, 259.

(28) Hollenstein, S.; Laube, T. *J. Am. Chem. Soc.* **1993**, *115*, 7240.

(29) (a) Sprow, F. B. *Ind. Eng. Chem. Process Des. Dev.* **1969**, *8*, 254−257. (b) Li, K. W.; Eckert, R. E.; Albright, L. F. *Ind. Eng. Chem. Process Des. Dev.* **1970**, *9*, 434.